Topics in Catalysis (2020) 63:810–816
https://doi.org/10.1007/s11244-020-01349-1

ORIGINAL PAPER

Formaldehyde Oxidation on Pd/TiO_2 Catalysts at Room Temperature: The Effects of Surface Oxygen Vacancies

Yaobin Li[1,2] · Chunying Wang[2,4] · Changbin Zhang[3,4] · Hong He[1,2,3,4]

Published online: 13 August 2020

Abstract
High reduction temperature generally induces the agglomeration of supported noble metals. Howerve, we found that high temperature reduction did not induce Pd particles sintering but improved Pd dispersion. Multiple methods were further carried out to illuminate the abnormal phenomenon. The results indicated more surface oxygen defects and diffusion of Pd particles were simultaneously induced by high temperature reduction. During diffusion process of Pd particles, they were trapped by the oxygen defects because of the strong metal-support interaction, which led to improvement of Pd dispersion on the Pd/TiO_2-450R catalyst. In addition, more surface oxygen vacancies on the Pd/TiO_2-450R catalyst resulted in more active sites of H_2O activation to form abundant surface OH groups which further enhanced adsorbed O_2 activation and mobility, and then opening a more effective pathway for HCHO oxidation, which result in its high activity of Pd/TiO_2-450R for ambient HCHO oxidation.

Keywords Oxygen vacancies · Dispersion · High temperature reduction · Formaldehyde · Catalytic oxidation

1 Introduction

Formaldehyde (HCHO), emitting from building/furnishing materials and decorative products, is one of the main indoor pollutants [1]. It is well known that HCHO is harmful to human health, leading to nasal tumors, headache, eye irritation, respiratory tract or even cancer [2]. With increasing attention paid on the pollution of HCHO, effective methods to remove indoor HCHO is of great importance for improving indoor air quality and reducing public health risks.

Several methods, such as adsorption [3], photo-catalysis [4] and catalytic oxidation [5] have been used to remove HCHO. In comparison, catalytic oxidation is widely recognized to be the promising method because HCHO oxidation could be effectively decomposed into harmless CO_2 and H_2O without any secondary pollution [6]. For decades, metal oxide catalysts (Ag, Mn, Co and Ni) [7–16] and supported noble metal (Pt, Au, Pd, Ir, Rh) catalysts [17–21] were attracting attention of researchers for HCHO oxidation. The former usually needed higher reaction temperature to completely decompose HCHO, while the later had shown excellent performance in HCHO oxidation at room temperature and thus was considered to be more suitable for indoor HCHO elimination. However, high cost of supported noble metal catalysts limited their wide application. Therefore, it is significant to lower application cost of supported noble metal catalysts by further improving their performance of HCHO oxidation.

As is well known, increasing the dispersion of supported noble metals is meaningful to improve the utilization of noble metals and increase the reaction active sites. Previously, we found that alkali metals addition could facilitate noble metals dispersion through strong promoter-metal interactions [21–23]. Besides, we also found high temperature reduction did not lead in agglomeration of Pd particles but

✉ Hong He
honghe@rcees.ac.cn

1 Ningbo Urban Environment Observation and Research Station, Institute of Urban Environment, Chinese Academy of Sciences, Ningbo 315800, China

2 Center for Excellence in Regional Atmospheric Environment, Key Laboratory of Urban Pollutant Conversion, Institute of Urban Environment, Chinese Academy of Sciences, Xiamen 361021, China

3 State Key Joint Laboratory of Environment Simulation and Pollution Control, Research Center for Eco-Environmental Sciences, Chinese Academy of Sciences, Beijing 100085, China

4 University of Chinese Academy of Sciences, Beijing 100049, China

did induce increasing of Pd dispersion, which was attributed to that TiO_{2-x}, formed at high temperature, diffused to the surface of Pd particles and then trapped them [24]. Whether is there other potential explanation to the abnormal phenomenon? It was reported that surface defects on carriers, such as step edges [25] or oxygen vacancies [26, 27], played important roles on trapping supported metals due to strong metal-support interactions. As we know, oxygen vacancies can be formed by high-temperature heating under ultra-high vacuum [28, 29] or reducing atmosphere [30], high-energy particle bombardment [31] and ion or γ-ray sputtering [32, 33], etc. The first method was regarded as a simple and effective way to produce oxygen vacancies, besides it may simultaneously induce supported metals diffusion and agglomeration. Thus, a conjecture that Pd particles were trapped by oxygen defects on TiO_2 during Pd particles diffusion process is worthy to be explored.

In this study, electron spin resonance (ESR), Fourier transform infrared of CO chemisorption (CO-FTIR), temperature-programmed reduction by CO (CO-TPR) and temperature-programmed desorption by O_2 (O_2-TPD) methods were further carried out to illuminate the abnormal phenomenon induced by high temperature reduction on Pd/TiO_2 catalysts. Based on the results of characterizations, the effect of oxygen vacancies on Pd dispersion and HCHO oxidation of Pd/TiO_2 catalysts was discussed.

2 Experimental

2.1 Catalyst Preparation

1 wt% Pd/TiO_2 was prepared by co-impregnation of TiO_2 with aqueous $Pd(NO_3)_2$, according to our previous study [20, 34]. Before activity testing and characterization, the samples were reduced with H_2 at 300 °C and 450 °C for 1 h, and denoted as Pd/TiO_2-300R and Pd/TiO_2-450R respectively.

2.2 Catalyst Characterization

X-band electron paramagnetic resonance (EPR) spectra were recorded at room temperature using a Bruker A300-10/12EPR spectrometer.

For Fourier transform infrared of CO chemisorption (CO-FTIR), the samples were first pre-reduced with H_2 at 300 °C or 450 °C for 1 h, followed by purging with He for 30 min to desorb H_2. Then the system was outgassed at 300 °C until $P = 10^{-3}$ torr for 30 min. Finally, the system was cooled down to the room temperature before introduction of CO (5% CO/He, P = 50 Torr) and IR measurements.

Temperature-programmed reduction by CO (CO-TPR) was conducted in a Micromeritics AutoChem II 2920 apparatus equipped with Mass detector. The samples were first pre-reduced with H_2 at 300 °C or 450 °C for 1 h, followed by purging with He for 30 min to desorb H_2. Then, the system was cooled down to 25 °C and the gas was switched to 5%O_2 and 1% H_2O for 30 min followed by He purging for 30 min. Finally, the gas was switched to 5%CO/He and the system was heated at a rate of 10 °C min^{-1}. Temperature-programmed desorption by O_2 (O_2-TPD) was conducted according to our previous work [34].

2.3 Catalyst Activity Testing

Catalyst activity testing for HCHO oxidation was performed according to our previous work [18]. For kinetics measurement, the feed gas composition was 300 ppm HCHO at a gas hourly space velocity of 300,000 h^{-1}. The reactor was operated in a differential mode, keeping the HCHO conversion below 20%. As a probe reaction, the activity tests for CO oxidation with or without water over Pd/TiO_2 catalysts (~ 15 mg) was performed in a fixed-bed quartz flow reactor. The feed gas flow is 100 ml min^{-1} containing 1% CO, 20% O_2 and 4% H_2O balanced by N_2. The CO and CO_2 were monitored by Shangfen GC-112A equipped with a TDX-01 column and hydrogen flame ionization detector (FID). Before activity testing, the catalysts were pre-reduced with H_2 flow at 300 or 450 °C for 1 h, followed by He flow purge at 300 °C for 30 min and then cooled down to room temperature.

3 Results and Discussion

3.1 Surface Oxygen Defects

The EPR technique was employed to characterize the defect structures of TiO_2 and Pd/TiO_2 catalysts and the result was shown in Fig. 1. There was no signal on the pure TiO_2, while an obvious signal at g = 2.005, which assigned to oxygen vacancies, appeared on Pd/TiO_2-300R and Pd/TiO_2-450R catalysts [35]. In comparison, the signal intensity became stronger after high temperature reduction, which indicated that there were more oxygen vacancies on Pd/TiO_2-450R catalyst than that on Pd/TiO_2-300R catalyst. It is well known that oxygen vacancies on TiO_2 are the important active sites of water dissociation to form surface hydroxyl groups [36, 37] which play essential roles in HCHO oxidation.

Structure properties of all samples were further examined by measuring Raman scattering. As shown in Fig. 2, Raman active modes locating at ~ 150 cm^{-1} (E_g), ~ 400 cm^{-1} (B_{1g}), ~ 520 cm^{-1} (B_{1g}) and ~ 640 cm^{-1} (E_g) were found on all samples and should be attributed to anatase phase [38]. Compared with TiO_2-300R, the main E_g mode of TiO_2-450R (locating at 147) became broaden after high temperature reduction. After Pd loading, the lowest frequency of E_g

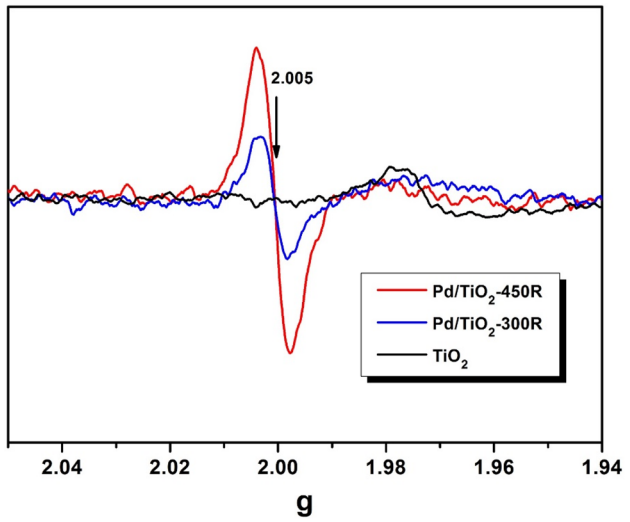

Fig. 1 EPR spectra on TiO_2, Pd/TiO_2-300R and Pd/TiO_2-450R samples

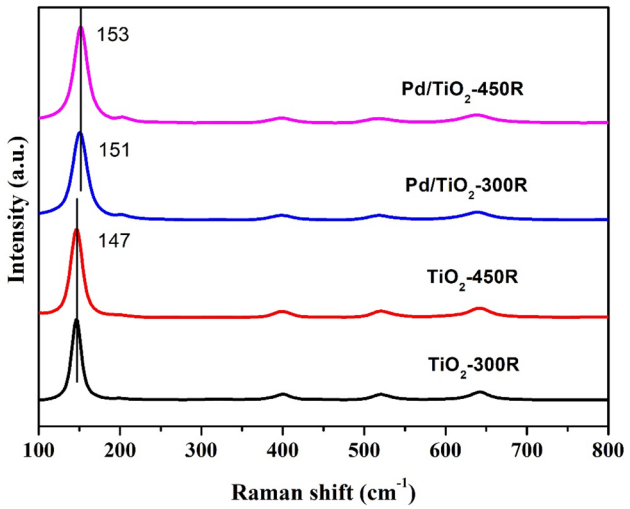

Fig. 2 Raman spectra of TiO_2 and Pd/TiO_2 samples

mode shifted to 151 and 153 cm^{-1} on Pd/TiO_2-300R and Pd/TiO_2-450R, respectively. The broadening and blue shift of E_g mode could be ascribed to the formation of oxygen vacancies on the samples surface during reduction, which was in line with the result of EPR.

3.2 Strong Metal-Support Interaction

As is well known that the SMSI usually results in the suppression of adsorption of small molecules such as CO and H_2 along with the electron transfer between metal and support [39–41]. CO-FTIR was next carried out to elucidate the SMSI on the Pd/TiO_2-300R and Pd/TiO_2-450R catalysts and the result was shown in Fig. 3. Three carbonyl bands

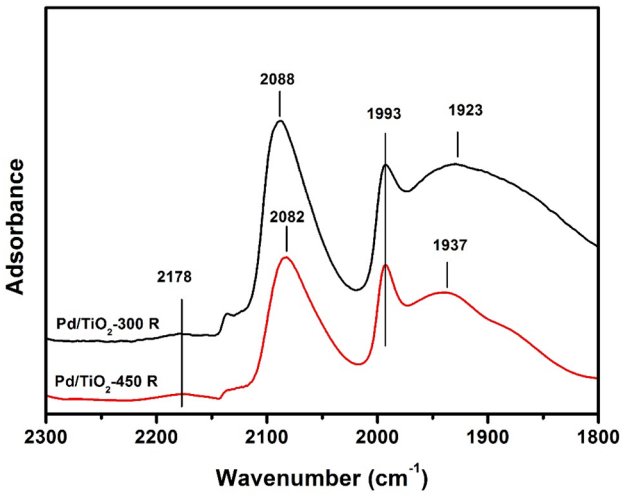

Fig. 3 IR spectra of CO (50 Torr) absorbed on Pd/TiO_2-300R and Pd/TiO_2-450R samples

of coordinated CO were detected on the reduced Pd/TiO_2 catalysts. The band at 2022–2160 cm^{-1} is assigned to the linear adsorbed CO on Pd, and the other band located at 1800–2022 cm^{-1} is assigned to the bridge bonded CO on Pd [42]. Compared to the Pd/TiO_2-300R catalyst, the intensity of adsorbed CO on the Pd/TiO_2-450R catalyst decreased, which can be attributed to the SMSI formed during high temperature reduction [39, 40, 43]. Meanwhile, the band shift of the linear CO stretching to lower wavenumber was also observed on the Pd/TiO_2-450R catalyst, which can be attributed to the increase of electronic density in the d subshell of Pd [41]. The phenomenon can also be demonstrated by the results of Pd 3d XPS in our previous work [24].

Combined with the result of EPR, the improvement of Pd dispersion on Pd/TiO_2-450R catalyst could be ascribed to that high temperature reduction simultaneously induced oxygen defects on TiO_2 surface and Pd particles diffusion to agglomeration. The Pd particles were trapped by oxygen defects during their diffusion process [26, 27].

3.3 Surface Oxygen Species

Furthermore, CO oxidation as a probe reaction was carried out to further verify the promotion effect of H_2O on the Pd/TiO_2-300R and Pd/TiO_2-450R catalysts and the result is shown in Fig. 4. When H_2O was absent in the system, the temperatures of 10%, 50% and 100% CO conversion for the Pd/TiO_2-300R catalyst were 38, 60 and 110 °C respectively, while they were 51, 85 and 155 °C for the Pd/TiO_2-450R catalyst. Based on the result, it is obvious that the Pd/TiO_2-300R catalyst possessed higher activity for CO oxidation than the Pd/TiO_2-450R catalyst, which may due to that, as is mentioned before, the CO adsorption weakened by SMSI on

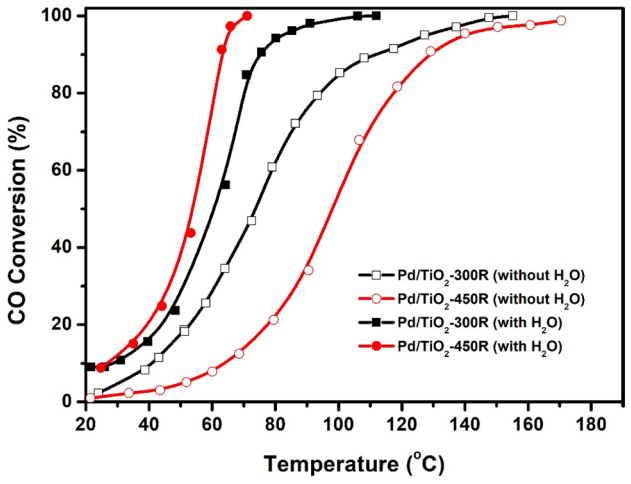

Fig. 4 The activity of CO oxidation on Pd/TiO_2-300R and Pd/TiO_2-450R catalysts. Reaction condition: 1% CO, 20% O_2, 4% H_2O balanced by N_2, GHSV = 40,000 mL g^{-1} h

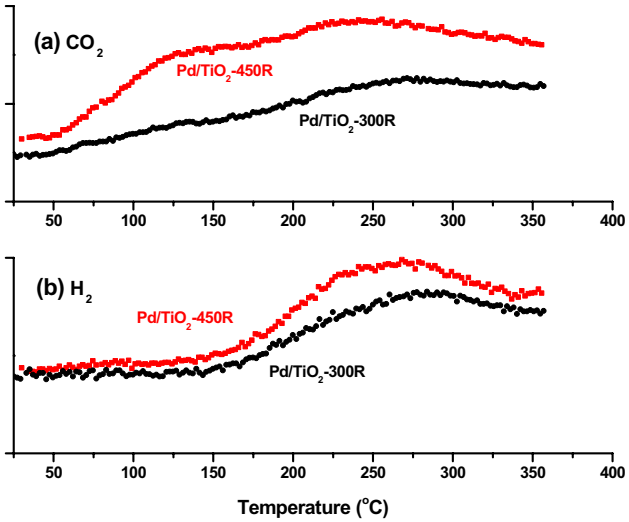

Fig. 5 CO-TPR profiles of Pd/TiO_2-300R and Pd/TiO_2-450R samples

the Pd/TiO_2-450R catalyst was unfavorable for CO oxidation [44]. In comparison, when 4% H_2O was added in the system, the temperature of 10%, 50% and 100% CO conversion were improved to 28, 60 and 106 °C for the Pd/TiO_2-300R catalyst and to 27, 53 and 71 °C for the Pd/TiO_2-450R catalyst. It is clear that the performance of Pd/TiO_2-300R and Pd/TiO_2-450R catalysts for CO oxidation was significantly improved. However, contrary to the above result, the Pd/TiO_2-450R catalyst showed a higher activity than Pd/TiO_2-300R catalyst for CO oxidation. According to the previous work, it is believed that surface OH groups formed by water dissociation on oxygen vacancies [45] or on metal surfaces through water-oxygen interaction [46–48] have a promotion effect on the supported Pt or Au catalysts for CO oxidation. Therefore, combined with the above results, it is reasonable to conclude that Pd/TiO_2-450R catalyst has a better ability of H_2O or H_2O/O_2 activation and possesses more surface active OH groups.

We also performed CO-TPR ($2CO + 2OH \rightarrow 2CO_2 + H_2$) to determine whether activation of the surface OH species was enhanced on the Pd/TiO_2-450R catalyst. As shown in Fig. 5, more H_2 and CO_2 were generated on the Pd/TiO_2-450R catalyst than on the Pd/TiO_2-300R catalyst, indicating that more active OH groups existed on the Pd/TiO_2-450R catalyst to react with CO to produce CO_2 and H_2. We previously have shown that surface OH groups play an important role in ambient HCHO oxidation since OH reaction with formate species to final products is a facile pathway for HCHO oxidation [24]. Therefore, the enhancement of the surface OH concentration by high temperature reduction is one of the main reasons for the improved performance of Pd/TiO_2-450R for HCHO oxidation. Furthermore, the OH species could facilitate O_2 adsorption and activation on TiO_2 (110) [49, 50] and enhance the diffusion of oxygen along the surface Ti (5c) to the metal-support interface where always be recognized as the active sites [50, 51].

O_2-TPD experiments were next performed to investigate the O_2 activation over the Pd/TiO_2-300R and Pd/TiO_2-450R catalysts and the profiles are shown in Fig. 6. There was only one broad O_2 desorption peak on both Pd/TiO_2-300R and Pd/TiO_2-450R catalysts in the temperature range of 25–400 °C. For Pd/TiO_2-300R catalyst, the O_2 desorption occurred at about 140 °C and the peak was centered at 230 °C. With higher temperature reduction, the O_2 desorption peak shifted to low temperature range, starting at about 80 °C and centering at 200 °C, indicating that mobility and activation of the chemisorbed oxygen were indeed enhanced on Pd/TiO_2-450R catalyst, which may

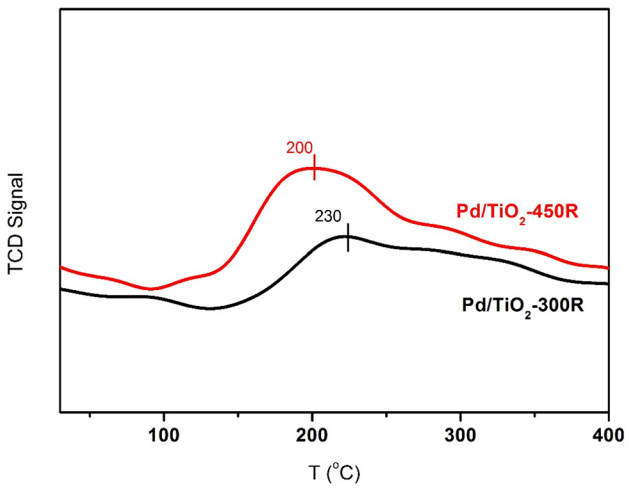

Fig. 6 O_2-TPD on Pd/TiO_2-300R and Pd/TiO_2-450R catalysts

contribute to its excellent performance of HCHO oxidation at room temperature.

3.4 Kinetics Test

To further check for the HCHO oxidation pathway, we carried out kinetics tests on the Pd/TiO_2 catalysts. Arrhenius-type plots for the rates of HCHO oxidation on the Pd/TiO_2-300R and Pd/TiO_2-450R catalysts are shown in Fig. 7. The apparent activation energy of the reaction on the Pd/TiO_2-300R catalyst is 153 kJ mol^{-1}, while it was lowered to about 50 kJ mol^{-1} on the Pd/TiO_2-450R catalyst. That is, the reaction was easier to activate on the Pd/TiO_2-450R catalyst, which is in line with the result of HCHO-TPD in our previous work [24].

3.5 Performance of HCHO Oxidation

The catalytic performance of the Pd/TiO_2-300R and Pd/TiO_2-450R catalyst was also checked by long isothermal tests under the same condition at 25 °C and the result was shown in Fig. 8. At the beginning of testing, both of the Pd/TiO_2 catalysts showed complete HCHO conversion. However, the HCHO conversion dropped slightly and was finally stable at 10% after 4 h, which may be attributed to that the consumed surface hydroxyl groups could not be effectively recovered on the Pd/TiO_2-300R catalyst due to its limited activation ability of H_2O. In comparison, the Pd/TiO_2-450R catalyst kept an obvious HCHO conversion for 13 h because of its excellent H_2O and O_2 activation ability.

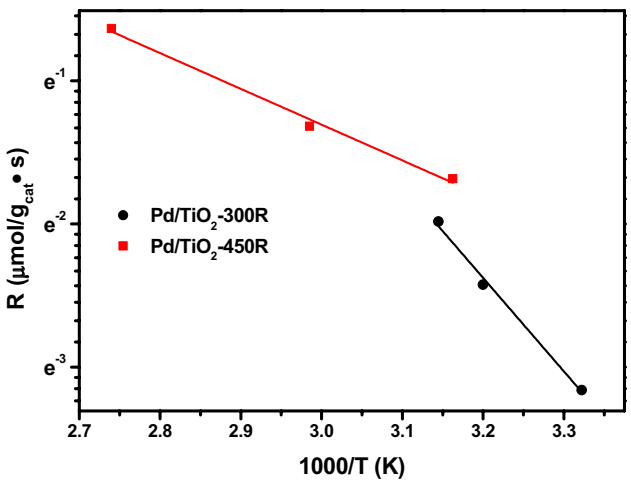

Fig. 7 HCHO oxidation rate R on Pd/TiO_2-300R and Pd/TiO_2-450R samples. Reaction condition: 300 ppm HCHO, 20% O_2, 2% H_2O and GHSV = 300000 h^{-1}

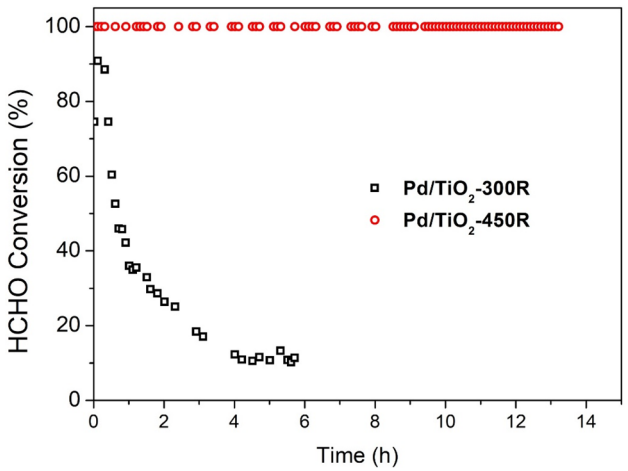

Fig. 8 Performance in HCHO oxidation of Pd/TiO_2-300R and Pd/TiO_2-450R samples. Reaction condition: 140 ppm HCHO, 20% O_2, 2% H_2O and GHSV = 95000 h^{-1}

4 Conclusions

It is found that high temperature reduction had a promotion effect on the Pd/TiO_2 for HCHO oxidation at room temperature. High temperature reduction induced surface oxygen defects and diffusion of Pd particles. Because of the strong metal-support interaction, the diffused Pd particles were trapped by the oxygen defects, which led to improvement of Pd dispersion on the Pd/TiO_2-450R catalyst. In addition, more surface oxygen vacancies on the Pd/TiO_2-450R catalyst resulted in more active sites of H_2O activation to form abundant surface OH groups which further enhanced adsorbed O_2 activation and mobility. In addition, lower apparent activation energy of HCHO oxidation on the Pd/TiO_2-450R catalyst made it to follow a more efficient reaction pathway of HCHO oxidation. Hence, the Pd/TiO_2-450R catalyst demonstrates a much higher activity than Pd/TiO_2-300R for HCHO oxidation at room temperature.

Acknowledgements This work was financially supported by the National Natural Science Foundation of China (Grant No. 21707136) and Natural Science Foundation of Fujian Province, China (Grant No. 2018J05027).

References

1. Zhang L, Jiang Y, Chen B-B, Shi C, Li Y, Wang C, Han S, Pan S, Wang L, Meng X, Xiao F-S (2019) Exceptional activity for formaldehyde combustion using siliceous Beta zeolite as a catalyst support. Catal Today. https://doi.org/10.1016/j.cattod.2019.01.016
2. Sun XC, Lin J, Guan HL, Li L, Sun L, Wang YH, Miao S, Su Y, Wang XD (2018) Complete oxidation of formaldehyde over TiO_2 supported subnanometer Rh catalyst at ambient temperature.

Appl Catal B 226:575–584. https://doi.org/10.1016/j.apcatb.2018.01.011
3. de Falco G, Li W, Cimino S, Bandosz TJ (2018) Role of sulfur and nitrogen surface groups in adsorption of formaldehyde on nanoporous carbons. Carbon 138:283–291. https://doi.org/10.1016/j.carbon.2018.05.067
4. Zhu M, Muhammad Y, Hu P, Wang B, Wu Y, Sun X, Tong Z, Zhao Z (2018) Enhanced interfacial contact of dopamine bridged melamine-graphene/TiO_2 nano-capsules for efficient photocatalytic degradation of gaseous formaldehyde. Appl Catal B 232:182–193. https://doi.org/10.1016/j.apcatb.2018.03.061
5. Fang RM, Huang HB, Ji J, He M, Feng QY, Zhan YJ, Leung DYC (2018) Efficient MnOx supported on coconut shell activated carbon for catalytic oxidation of indoor formaldehyde at room temperature. Chem Eng J 334:2050–2057. https://doi.org/10.1016/j.cej.2017.11.176
6. Quiroz Torres J, Royer S, Bellat JP, Giraudon JM, Lamonier JF (2013) Formaldehyde: catalytic oxidation as a promising soft way of elimination. Chemsuschem 6(4):578–592. https://doi.org/10.1002/cssc.201200809
7. Bai BY, Li JH (2014) Positive Effects of K^+ Ions on Three-Dimensional Mesoporous Ag/Co_3O_4 Catalyst for HCHO Oxidation. ACS Catal 4(8):2753–2762. https://doi.org/10.1021/Cs5006663
8. Du X, Li C, Zhao L, Zhang J, Gao L, Sheng J, Yi Y, Chen J, Zeng G (2018) Promotional removal of HCHO from simulated flue gas over Mn–Fe oxides modified activated coke. Appl Catal B 232:37–48. https://doi.org/10.1016/j.apcatb.2018.03.034
9. Tang XF, Chen JL, Huang XM, Xu YD, Shen WJ (2008) Pt/MnO_x–CeO_2 catalysts for the complete oxidation of formaldehyde at ambient temperature. Appl Catal B 81(1–2):115–121. https://doi.org/10.1016/j.apcatb.2007.12.007
10. Tang XF, Li YG, Huang XM, Xu YD, Zhu HQ, Wang JG, Shen WJ (2006) MnOx–CeO_2 mixed oxide catalysts for complete oxidation of formaldehyde: effect of preparation method and calcination temperature. Appl Catal B-Environ 62(3–4):265–273. https://doi.org/10.1016/j.apcatb.2005.08.004
11. Wang M, Zhang L, Huang W, Xiu T, Zhuang C, Shi J (2017) The catalytic oxidation removal of low-concentration HCHO at high space velocity by partially crystallized mesoporous MnOx. Chem Eng J 320:667–676. https://doi.org/10.1016/j.cej.2017.03.098
12. Liu F, Rong S, Zhang P, Gao L (2018) One-step synthesis of nanocarbon-decorated MnO_2 with superior activity for indoor formaldehyde removal at room temperature. Appl Catal B 235:158–167. https://doi.org/10.1016/j.apcatb.2018.04.078
13. Zhu L, Wang J, Rong S, Wang H, Zhang P (2017) Cerium modified birnessite-type MnO_2 for gaseous formaldehyde oxidation at low temperature. Appl Catal B 211:212–221. https://doi.org/10.1016/j.apcatb.2017.04.025
14. Fan Z, Shi J, Zhang Z, Chen M, Shangguan W (2018) Promotion effect of potassium carbonate on catalytic activity of Co_3O_4 for formaldehyde removal. J Chem Technol Biotechnol 93(12):3562–3568. https://doi.org/10.1002/jctb.5733
15. Wang HC, Guo WQ, Jiang Z, Yang R, Jiang Z, Pan Y, Shangguan WF (2018) New insight into the enhanced activity of ordered mesoporous nickel oxide in formaldehyde catalytic oxidation reactions. J Catal 361:370–383. https://doi.org/10.1016/j.jcat.2018.02.023
16. Bai BY, Arandiyan H, Li JH (2013) Comparison of the performance for oxidation of formaldehyde on nano-Co_3O_4, 2D-Co_3O_4, and 3D-Co_3O_4 catalysts. Appl Catal B 142:677–683. https://doi.org/10.1016/j.apcatb.2013.05.056
17. Yan Z, Xu Z, Cheng B, Jiang C (2017) Co_3O_4 nanorod-supported Pt with enhanced performance for catalytic HCHO oxidation at room temperature. Appl Surf Sci 404:426–434. https://doi.org/10.1016/j.apsusc.2017.02.010
18. Li YB, Chen XY, Wang CY, Zhang CB, He H (2018) Sodium enhances Ir/TiO_2 activity for catalytic oxidation of formaldehyde at ambient temperature. ACS Catal 8(12):11377–11385. https://doi.org/10.1021/acscatal.8b03026
19. Ma C, Wang D, Xue W, Dou B, Wang H, Hao Z (2011) Investigation of formaldehyde oxidation over Co_3O_4–CeO_2 and Au/Co_3O_4–CeO_2 catalysts at room temperature: effective removal and determination of reaction mechanism. Environ Sci Technol 45(8):3628–3634. https://doi.org/10.1021/es104146v
20. Li YB, Zhang CB, He H, Zhang JH, Chen M (2016) Influence of alkali metals on Pd/TiO_2 catalysts for catalytic oxidation of formaldehyde at room temperature. Catal Sci Technol 6(7):2289–2295. https://doi.org/10.1039/C5CY01521A
21. Zhang CB, Liu FD, Zhai YP, Ariga H, Yi N, Liu YC, Asakura K, Flytzani-Stephanopoulos M, He H (2012) Alkali-metal-promoted Pt/TiO_2 opens a more efficient pathway to formaldehyde oxidation at ambient temperatures. Angew Chem Int Ed 51(38):9628–9632. https://doi.org/10.1002/anie.201202034
22. Zhai Y, Pierre D, Si R, Deng W, Ferrin P, Nilekar AU, Peng G, Herron JA, Bell DC, Saltsburg H, Mavrikakis M, Flytzani-Stephanopoulos M (2010) Alkali-stabilized Pt-OH_x species catalyze low-temperature water-gas shift reactions. Science 329(5999):1633. https://doi.org/10.1126/science.1192449
23. Yang M, Li S, Wang Y, Herron JA, Xu Y, Allard LF, Lee S, Huang J, Mavrikakis M, Flytzani-Stephanopoulos M (2014) Catalytically active Au-O(OH)x- species stabilized by alkali ions on zeolites and mesoporous oxides. Science 346(6216):1498. https://doi.org/10.1126/science.1260526
24. Li Y, Zhang C, Ma J, Chen M, Deng H, He H (2017) High temperature reduction dramatically promotes Pd/TiO_2 catalyst for ambient formaldehyde oxidation. Appl Catal B 217:560–569. https://doi.org/10.1016/j.apcatb.2017.06.023
25. Jones J, Xiong H, DeLaRiva AT, Peterson EJ, Pham H, Challa SR, Qi G, Oh S, Wiebenga MH, Pereira Hernández XI, Wang Y, Datye AK (2016) Thermally stable single-atom platinum-on-ceria catalysts via atom trapping. Science 353(6295):150. https://doi.org/10.1126/science.aaf8800
26. Sanchez MG, Gazquez JL (1987) Oxygen vacancy model in strong metal-support interaction. J Catal 104(1):120–135. https://doi.org/10.1016/0021-9517(87)90342-3
27. Jiawei Wan WC, Jia C, Zheng L, Dong J, Xusheng Zheng Yu, Wang WY, Chen C, Peng Q, Wang D, Li Y (2018) Defect effects on TiO_2 nanosheets: stabilizing single atomic site Au and promoting catalytic properties. Adv Mater 8:1705369–1705377. https://doi.org/10.1002/adma.201705369
28. Pan X, Yang M-Q, Fu X, Zhang N, Xu Y-J (2013) Defective TiO_2 with oxygen vacancies: synthesis, properties and photocatalytic applications. Nanoscale 5:3601–3614. https://doi.org/10.1039/c3nr00476g
29. Pan J-M, Maschhoff BL, Diebold U, Madey TE (1992) Interaction of water, oxygen, and hydrogen with TiO_2(110) surfaces having different defect densities. J Vac Sci Technol A 10:7. https://doi.org/10.1116/1.577986
30. Li Y, Xu B, Fan Y, Feng N, Qiu A, He JMJ, Yang H, Chen Y (2004) The effect of titania polymorph on the strong metal-support interaction of Pd/TiO_2 catalysts and their application in the liquid phase selective hydrogenation of long chain alkadienes. J Mol Catal A 216(1):107–114. https://doi.org/10.1016/j.molcata.2004.02.007
31. Bromiley GD, Shiryaev AA (2006) Neutron irradiation and post-irradiation annealing of rutile (TiO_{2-x}): effect on hydrogen incorporation and optical absorption. Phys Chem Miner 33(6):426–434. https://doi.org/10.1007/s00269-006-0087-9
32. Wang L-Q, Baer DR, Engelhard MH, Shultz AN (1995) The adsorption of liquid and vapor water on TiO_2(110)

surfaces: the role of defects. Surf Sci 344(3):237–250. https://doi.org/10.1016/0039-6028(95)00859-4
33. Dutta PK, Ginwalla A, Hogg B, Patton BR, Chwieroth B, Liang Z, Gouma P, Mills M, Akbar S (1999) Interaction of carbon monoxide with anatase surfaces at high temperatures: optimization of a carbon monoxide sensor. J Phys Chem B 103(21):4412–4422. https://doi.org/10.1021/jp9844718
34. Zhang CB, Li YB, Wang YF, He H (2014) Sodium-promoted Pd/TiO_2 for catalytic oxidation of formaldehyde at ambient temperature. Environ Sci Technol 48(10):5816–5822. https://doi.org/10.1021/Es4056627
35. Li J, Zhang M, Guan Z, Li Q, He C, Yang J (2017) Synergistic effect of surface and bulk single-electron-trapped oxygen vacancy of TiO_2 in the photocatalytic reduction of CO_2. Appl Catal B 206:300–307. https://doi.org/10.1016/j.apcatb.2017.01.025
36. Brookes IM, Muryn CA, Thornton G (2001) Imaging water dissociation on TiO_2(110). Phys Rev Lett 87(26):266103. https://doi.org/10.1103/PhysRevLett.87.266103
37. Schaub R, Thostrup P, Lopez N, Lægsgaard E, Stensgaard I, Nørskov JK, Besenbacher F (2001) Oxygen vacancies as active sites for water dissociation on rutile TiO_2(110). Phys Rev Lett 87(26):266104. https://doi.org/10.1103/PhysRevLett.87.266104
38. Zeng L, Song WL, Li MH, Zeng DW, Xie CS (2014) Catalytic oxidation of formaldehyde on surface of $HTiO_2$/$HCTiO_2$ without light illumination at room temperature. Appl Catal B 147:490–498. https://doi.org/10.1016/j.apcatb.2013.09.013
39. Tauster SJ, Fung SC, Garten RL (1978) Strong metal-support interactions Group 8 Noble metals supported on TiO_2. J Am Chem Soc 100(1):170–175. https://doi.org/10.1021/Ja00469a029
40 Vannice MA, Twu CC, Moon SH (1983) SMSI effects on CO adsorption and hydrogenation on Pt catalysts: I. Infrared spectra of adsorbed CO prior to and during reaction conditions. J Catal 79(1):70–80. https://doi.org/10.1016/0021-9517(83)90290-7
41. Benvenutti EV, Franken L, Moro CC, Davanzo CU (1999) FTIR study of hydrogen and carbon monoxide adsorption on Pt/TiO_2, Pt/ZrO_2, and Pt/Al_2O_3. Langmuir 15(23):8140–8146. https://doi.org/10.1021/La990195s
42. Sheu LL, Sachtler WMH (1993) Detection by CO-FTIR of incipient metal—support interaction in Rh/SiO_2 and Pd/TiO_2. J Mol Catal 81(2):267–278. https://doi.org/10.1016/0304-5102(93)80011-I
43. Sá J, Bernardi J, Anderson J (2007) Imaging of low temperature induced SMSI on Pd/TiO_2 catalysts. Catal Lett 114(1–2):91–95. https://doi.org/10.1007/s10562-007-9049-1
44. Zhu HQ, Qin ZF, Shan WJ, Shen WJ, Wang JW (2005) Low-temperature oxidation of CO over Pd/CeO_2–TiO_2 catalysts with different pretreatments. J Catal 233(1):41–50. https://doi.org/10.1016/j.jcat.2005.04.033
45. Zhang Z, Bondarchuk O, Kay BD, White JM, Dohnalek Z (2006) Imaging water dissociation on TiO_2 (110): evidence for inequivalent geminate OH groups. J Phys Chem B 110(43):21840–21845. https://doi.org/10.1021/Jp063619h
46. Ojifinni RA, Froemming NS, Gong J, Pan M, Kim TS, White JM, Henkelman G, Mullins CB (2008) Water-enhanced low-temperature CO oxidation and isotope effects on atomic oxygen-covered Au(111). J Am Chem Soc 130(21):6801–6812. https://doi.org/10.1021/ja800351j
47. Bongiorno A, Landman U (2005) Water-enhanced catalysis of CO oxidation on free and supported gold nanoclusters. Phys Rev Lett 95(106102):1–4. https://doi.org/10.1103/PhysRevLett.95.106102
48. Kim TS, Gong J, Ojifinni RA, White JM, Mullins CB (2006) Water activated by atomic oxygen on Au(111) to oxidize CO at low temperatures. J Am Chem Soc 128(19):6282–6283. https://doi.org/10.1021/ja058263m
49. Huang HB, Leung DYC (2011) Complete oxidation of formaldehyde at room temperature using TiO_2 supported metallic Pd nanoparticles. ACS Catal 1(4):348–354. https://doi.org/10.1021/cs200023p
50. Liu LM, McAllister B, Ye HQ, Hu P (2006) Identifying an O_2 supply pathway in CO oxidation on Au/TiO_2 (110): a density functional theory study on the intrinsic role of water. J Am Chem Soc 128(12):4017–4022. https://doi.org/10.1021/Ja056801p
51. Ammal SC, Heyden A (2014) Water-gas shift catalysis at corner atoms of Pt clusters in contact with a TiO_2 (110) support surface. ACS Catal 4(10):3654–3662. https://doi.org/10.1021/cs5009706